

Enhanced resistive switching effect in Ag nanoparticle embedded BaTiO₃ thin films

K. Au, X. S. Gao, Juan Wang, Z. Y. Bao, J. M. Liu et al.

Citation: *J. Appl. Phys.* **114**, 027019 (2013); doi: 10.1063/1.4812219

View online: <http://dx.doi.org/10.1063/1.4812219>

View Table of Contents: <http://jap.aip.org/resource/1/JAPIAU/v114/i2>

Published by the **AIP Publishing LLC**.

Additional information on *J. Appl. Phys.*

Journal Homepage: <http://jap.aip.org/>

Journal Information: http://jap.aip.org/about/about_the_journal

Top downloads: http://jap.aip.org/features/most_downloaded

Information for Authors: <http://jap.aip.org/authors>

ADVERTISEMENT



AIP Advances

Now Indexed in Thomson Reuters Databases

Explore AIP's open access journal:

- Rapid publication
- Article-level metrics
- Post-publication rating and commenting

Enhanced resistive switching effect in Ag nanoparticle embedded BaTiO₃ thin films

K. Au,¹ X. S. Gao,^{1,2} Juan Wang,¹ Z. Y. Bao,¹ J. M. Liu,² and J. Y. Dai^{1,a)}

¹Department of Applied Physics, The Hong Kong Polytechnic University (Shenzhen Research Institute), Hong Kong

²Institute for Advanced Materials, South China Normal University, Guangzhou, People's Republic of China

(Received 31 December 2012; accepted 7 March 2013; published online 10 July 2013)

Ag nanoparticle (NP) embedded BaTiO₃ (BTO) thin films on SrRuO₃-coated SrTiO₃ (STO) substrates are prepared by the integrated nanocluster beam deposition and laser-molecular beam epitaxy. Enhanced resistive switching, up to an ON/OFF ratio of 10⁴, has been achieved at low switching voltage (less than 1 V) without a forming voltage. These characteristics make such nanocomposite film very promising for application of low voltage non-volatile random access memory. The enhanced resistive switching effect may be attributed to the charge storage effect of the Ag nanoparticles and easy formation of Ag filament inside the BTO film. © 2013 AIP Publishing LLC.

[<http://dx.doi.org/10.1063/1.4812219>]

I. INTRODUCTION

Study of resistive switching toward application in resistive random-access memory (RRAM) has attracted a great deal of attention due to its promising in terms of high memory cell density and high ON/OFF (high resistance to low resistance) ratio as well as low leakage current compared to flash memory and phase change memory. However, unclear switching mechanism and unstable switching voltage are obstacles for real application of RRAM. Recently, ultrathin ferroelectric tunnel junction (FTJ) sandwiched by two metal layers with the ferroelectric layer as tunnel barrier is becoming an interesting topic, owing to their unique electron transport properties (e.g., giant electroresistance) and application potentials in ultrahigh density recording.^{1–3} However, it is challenging to obtain such kind of tunneling effect, which requires to maintain perfect ferroelectricity at nanometer scale of film thickness which is closing to the polarization vanishing critical thickness. The relatively lower ON/OFF ratio, up to 2–3 orders of magnitude,^{4–9} and large leakage current due to its extremely thin film thickness make the ferroelectric switching based RRAM immature and far from real application.

Lee *et al.* have demonstrated in one of their work that RRAM devices based on layer-by-layer structure, with Pt nanoparticle (NP) embedded in TiO₂ nanocomposite multilayers, achieved resistive switching properties with low operating voltages and large ON/OFF ratio of 10⁴ which is much higher than what has been achieved by the ferroelectric tunneling effect.¹⁰ The memory effect in the high and low current states can occur from charge storage (high resistance) and release (low resistance) within the charge trap sites. These results demonstrated the advantages of PtNP-embedded TiO₂ multilayers over the pure TiO₂ multilayers in electrical performance, and these enhanced memory properties were attributed to the presence of metal nanoparticles operating as deep charge trap sites.

Very recently, we found another interesting phenomenon when we embedded Ag nanoparticles into BaTiO₃ (BTO) films to form a particle/matrix nanocomposite by co-depositing the BTO film and Ag nanoparticles using a pulsed laser deposition system (PLD) equipped with a nanocluster beam generator. A very large electroresistance of 10⁴, which is larger than all the other reported FTJ, has been observed. Enlightened by this observation, in this work, we construct a novel ferroelectric film-metal nanoparticle nanocomposite and study its resistive switching characteristics. Study of this nanocomposite film system may lead to more rich physics, such as resonant tunneling (suggested by the presence of steps and peaks in the I-V curve) and new function of devices. In this paper, we report the fabrication and the resistive switching properties of the Ag nanoparticle embedded BTO film.

II. EXPERIMENT

The nanocomposite film was grown by co-deposition of BTO film and Ag nanoparticles using PLD system combined with a nanocluster generator. The BTO film was deposited by the PLD system at deposition temperature of 700–750 °C and in a high vacuum condition of around 10^{−4} Pa. The Ag nanoparticles were produced by an Ag nanocluster beam source, where an Ag target was magnetron sputtered and the Ag nanoclusters were formed by aggregation of Ag atoms in Ar gas, while an Ag nanocluster beam was formed and the Ag NPs fly through an aperture toward the substrate driven by the force of pressure gradient from the PLD to the magnetron sputter chamber. These Ag NPs were therefore embedded inside the BTO thin films.

To characterize the nanocomposite BTO/Ag NPs film's electrical properties, a thin layer of conductive SrRuO₃ (SRO ~ 15 nm) was deposited on SrTiO₃ (STO) substrate as bottom electrode, and Au electrodes of around 100 μm in diameter were used as top electrodes. Current-voltage characteristics of the film were characterized by a Keithley power source meter (2400), and surface topology of the film was characterized by a Veeco scanning probe microscope. Cross-sectional microstructure of the film was studied by

^{a)}Author to whom correspondence should be addressed. Electronic mail: jiyan.dai@polyu.edu.hk.

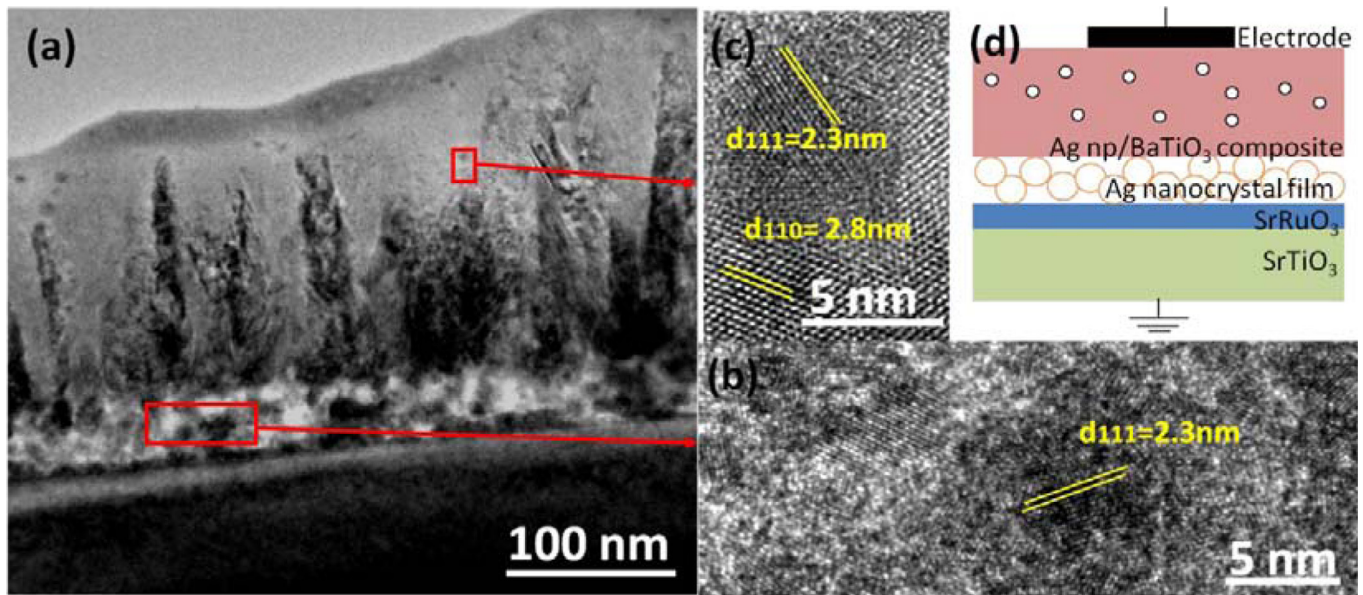


FIG. 1. (a) TEM image of the Ag NP embedded BTO composite film on STO substrate. Different layers are illustrated, i.e., a thin SrRuO₃ layer, Ag NP formed electrode layer, and Ag NPs/BaTiO₃ composite film; (b) High-resolution TEM images from the Ag NPs layer; (c) a typical Ag NP embedded in BaTiO₃ matrix; and (d) schematic diagram of the film structure.

high-resolution transmission electron microscopy (TEM, JOEL 2100F).

III. RESULTS AND DISCUSSION

Figure 1 shows microstructure and schematic diagram of the BTO/AgNPs nanocomposite film. From the low magnification TEM image (Figure 1(a)), it can be seen that the BTO film is about 200 nm thick and mainly composed of column-like BTO grains with dark-contrast particles embedded, while a layer with polycrystalline nanoparticles can be observed at the bottom of the BTO film. High-resolution TEM image of the polycrystalline nanoparticle layer (Figure 1(b)) shows that this layer is mainly composed of Ag nanoparticles with diameters ranging from 10 to 25 nm. However, smaller particles (~5-10 nm) with a relatively lower density are found embedded in the BTO film. Lattice fringes of the Ag NPs can be identified close to a BTO crystal from the high-resolution TEM image as shown in Fig. 1(c). Based on the TEM observation results, Fig. 1(d) schematically

illustrates the whole structure of the BTO/Ag NPs nanocomposite film and electrode on STO substrate.

In Fig. 2, energy dispersive x-ray (EDX) spectra taken from the nanoparticles and the matrix area of the composite film further confirm that Ag nanoparticles are embedded in the BTO film with rather low density. The non-uniform distribution of Ag nanoparticles in the composite film and on substrate can be attributed to the pressure change of the growth chamber during the PLD deposition. At the beginning of the growth, the nanoclusters beam source opens first, and the Ag NPs are deposited quickly, while when the PLD is started, the relatively higher kinetic energy of the BTO particles in the PLD plasma plume collide and scatter the Ag nanoparticles and results in a low deposition rate of Ag NPs with smaller size in the BTO film.

Figure 3(a) presents I-V curves of the Ag NP embedded BTO nanocomposite film showing characteristic hysteresis loop, where the high and low resistance states have a ratio of 10⁴. At the low voltage regime, the film is in an insulating state, while as the external voltage increases from zero and

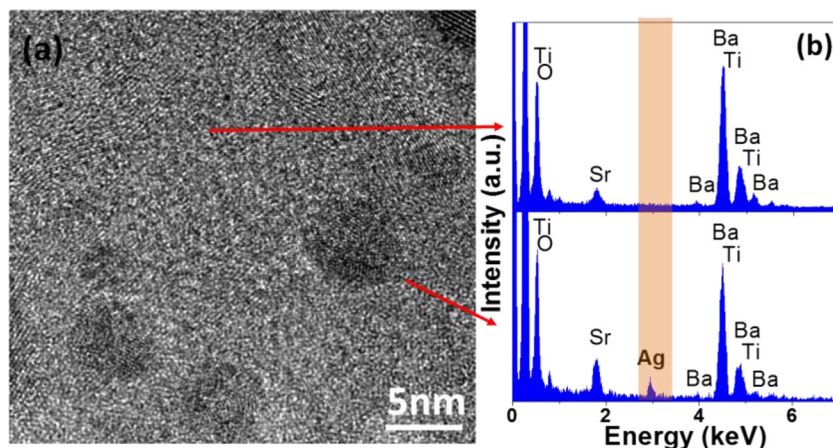


FIG. 2. (a) High-resolution TEM image of the Ag NP embedded BaTiO₃ composite layer and (b) the corresponding EDX spectra taken from the matrix and the nanoparticles.

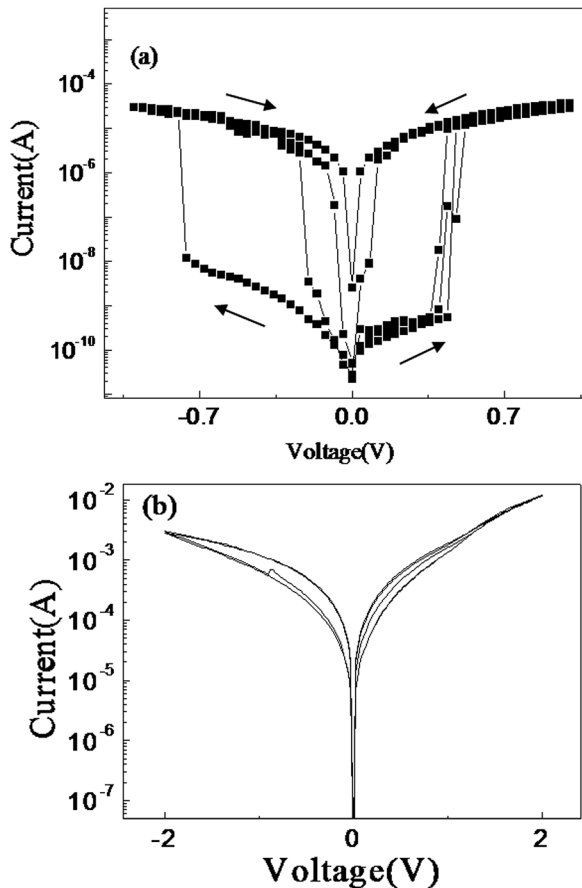


FIG. 3. (a) Unipolar resistance switching behavior of the Au/BTO-AgNPs/Ag device; (b) low resistive switching behavior of BaTiO₃ film without Ag NPs.

reaches a threshold voltage V_{SET} , a sudden decrease of resistance occurs. The low and high resistance states (HRSs) represent ON and OFF states, respectively. The much lower current even at low resistance state (LRS) promises the application potential as non-volatile memory. These results demonstrate that RRAM devices based on Ag NP embedded BTO film can have a unipolar switching property with low operating voltage and large ON/OFF ratio (10^4). It is worth noting that the capacitor of pure BTO film without Ag NPs exhibits very low ON/OFF ratio (<10 , Fig. 3(b)). The large ON/OFF ratio is also much larger than that of BTO based tunneling junction (~ 100).¹¹ It is, therefore, obvious that the incorporation of nanocomposite structures significantly enhances the ON/OFF ratio. More interestingly, the resistive switching occurs at bias as low as 1 V, without a forming process by large voltage, which is usually required by most resistive switching system.^{12–14} This is very promising for RRAM memories with ultralow operation bias.

The nanocomposite structure also exhibits unipolar resistive switching behavior at higher voltages. Figure 4 shows the typical unipolar switching characteristics for the Ag NP/BTO film when the sweep voltage increases to a few volts, where the I-V curve is shown in Fig. 4(a), and the R-V curve is shown in Fig. 4(b). One can see that as the external voltage V_{ext} increases from zero and reaches a threshold voltage V_{SET} , a sudden current increase occurs and the film changes from a HRS to a LRS. It is interesting to see that the HRS and

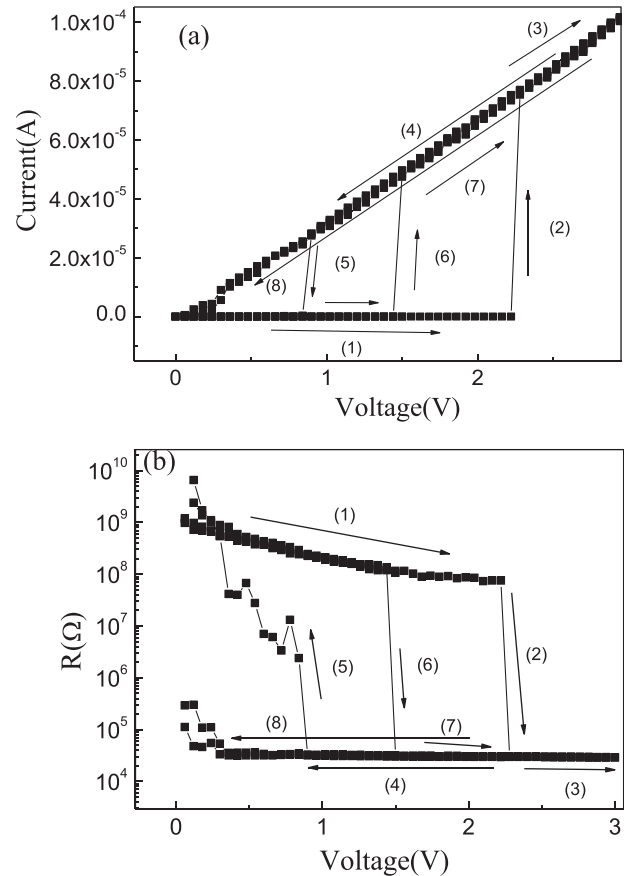


FIG. 4. Resistance switching of the Au/BTO-AgNPs/Ag device: (a) I-V curve and (b) R-V curve.

LRS are metastable and can suddenly switch from one to the other at a certain voltage. Although distributions occur in V_{RESET} and V_{SET} , one can see that the resistance changes at different V_{RESET} and V_{SET} are the same, i.e., the universal resistance change. These LRS and HRS can be used as the binary states for memory applications, and the large ON/OFF ratio and low current are promising characteristics for RRAM application. Compared to other resistive switching systems, the V_{RESET} and V_{SET} of our sample occur at relatively low voltages without a forming process.

It should be noted that the trace 5 in Fig. 4 indicates a fact that the low resistance state returns to high-resistance state when the voltage reduces to zero. However, if we look at the traces from 6 to 8, it shows that at zero voltage, the low resistance state can be retained. The uncertainty of switching voltage is a common issue in many resistive switching memories, and the wide distribution of V_{RESET} and V_{SET} is considered to be the major obstacle to practical RRAM applications. This issue could be more serious for the current sample, and more work is needed to study its retention and endurance properties.

Nevertheless, in this work, we emphasize the Ag nanoparticle induced giant resistive switching and quantum effect. The above giant ON/OFF ratio compared to the bare BTO film is believed to be due to the presence of Ag nanoparticle electrode and nanoparticles inside the film, resulting in a charging and discharging effect on the nanoparticles as well as easy formation of filaments. At relatively lower voltage

range, the I-V curves exhibit a characteristic of large and reversible current rectification behavior (Figure 3(a)), which is likely due to the charge and discharge of electrons inside the embedded Ag nanodots.^{10,15} In addition, we further attribute the wide distribution of the set and reset voltages to the Ag NP's quantum confinement and Coulomb blockade effect. It has also been reported that the volatile electrode of Ag NPs results in easy formation of the Ag filament inside oxide films through ion diffusion mechanism, while the Ag nanodots inside the Ag film should enhance this process. At higher voltages, filament effects become more significant, as demonstrated by the unipolar resistive switching behavior in Fig. 4, in which the I-V behavior at LRS state is like an Ohmic contact, implying the formation of a metal-like channels, e.g., Ag filament. In a general case, the I-V behavior should be governed by both the trapped and detrapped charges as well as filament effects. Further more, by detailed examination of Fig. 4(b), we can see that at the lower voltage range, multiple steps appear and the heights of the steps are about the same. This is similar to what has been called quantized conductance as reported in Ref. 16 due to the formation of multiple filaments. It is also worth noting that the ferroelectric switching induced resistive switching may also contribute to the large resistive switching, but further study is needed to understand this point.

IV. CONCLUSION

In conclusion, we have fabricated Ag NP embedded BTO nano-composite films and demonstrated that the resistive switching memory behavior based on the Ag NP embedded BTO film has unipolar switching property with low operating voltages and large ON/OFF ratios (10^4). The mechanism for this giant resistive switching is attributed to charge storage effect of Ag NPs as well as Ag NP electrode induced easy formation of filament inside the BTO film.

ACKNOWLEDGMENTS

This research was supported by the National key Basic Research Program of China (973 Program) under Grant No. 2013CB632900. The authors gratefully acknowledge financial support from the Hong Kong Research Grant Council (No. PolyU 514512). The author X.S.G also likes to acknowledge the Natural Science Foundation of China (Grant Nos. 51072061 and 51031004) for financial assist.

- ¹L. Esaki, R. B. Laibowitz, and P. J. Stiles, *IBM Tech. Discl. Bull.* **13**, 2161 (1971).
- ²E. Y. Tsymlal and H. Kohlstedt, *Science* **313**, 181 (2006).
- ³M. Dawber, K. M. Rabe, and J. F. Scott, *Rev. Mod. Phys.* **77**, 1083 (2005).
- ⁴J. Rodriguez Contreras, H. Kohlstedt, U. Roppe, R. Waser, C. Buchal, and N. A. Pertsev, *Appl. Phys. Lett.* **83**, 4595 (2003).
- ⁵V. Garcia, S. Fusil, K. Bouzouane, S. Enouz-Vedrenne, N. D. Mathur, A. Barthélémy, and M. Bibes, *Nature* **460**, 81 (2009).
- ⁶M. Hambe, A. Petraru, N. A. Pertsev, P. Munroe, V. Nagarajan, and H. Kohlstedt, *Adv. Funct. Mater.* **20**, 2436 (2010).
- ⁷A. Crassous, V. Garcia, K. Bouzouane, S. Fusil, A. H. G. Vlooswijk, G. Rispens, B. Noheda, M. Bibes, and A. Barthélémy, *Appl. Phys. Lett.* **96**, 042901 (2010).
- ⁸M. Gajek, M. Bibes, S. Fusil, K. Bouzouane, J. Fontcuberta, A. E. Barthelemy, and A. Fert, *Nature Mater.* **6**, 296 (2007).
- ⁹V. Garcia, M. Bibes, L. Bocher, S. Valencia, F. Kronast, A. Crassous, X. Moya, S. Enouz-Vedrenne, A. Gloter, D. Imhoff, C. Deranlot, N. D. Mathur, S. Fusil, K. Bouzouane, and A. Barthélémy, *Science* **327**, 1106 (2010).
- ¹⁰C. Lee, I. Kim, H. Shin, S. Kim, and J. Cho, *Nanotechnology* **21**, 185704 (2010).
- ¹¹X. S. Gao, J. M. Liu, K. Au, and J. Y. Dai, *Appl. Phys. Lett.* **101**, 142905-09 (2012).
- ¹²Z. B. Yan, Y. Y. Guo, G. Q. Zhang, and J.-M. Liu, *Adv. Mater.* **23**, 1351 (2011).
- ¹³R. Waser and M. Aono, *Nature Mater.* **6**, 833 (2007).
- ¹⁴K. Shibuya, R. Dittmann, S. Mi, and R. Waser, *Adv. Mater.* **22**, 411 (2010).
- ¹⁵X. Zou, H. G. Ong, L. You, W. G. Chen, H. Ding, H. Funakubo, L. Chen, and J. L. Wang, *AIP Adv.* **2**, 032166 (2012).
- ¹⁶X. J. Zhu, W. J. Su, Y. W. Liu, B. L. Hu, L. Pan, W. Lu, J. D. Zhang, and R.-W. Li, *Adv. Mater.* **24**, 3941 (2012).